HHS Public Access

Author manuscript

Arthritis Rheumatol. Author manuscript; available in PMC 2017 January 01.

Published in final edited form as:

Arthritis Rheumatol. 2016 January ; 68(1): 210–217. doi:10.1002/art.39421.

Endothelial cells expressing endothelial and mesenchymal cell gene products in Systemic Sclerosis-associated interstitial lung disease lung tissues

Fabian A. Mendoza, M.D.[1,2,5], **Sonsoles Piera-Velazquez, Ph.D.**[2,5], **John L. Farber, M.D.**[3], **Carol Feghali-Bostwick, Ph.D.**[4], and **Sergio A. Jimenez, M.D.**[2]

[1]Division of Rheumatology, Department of Medicine, Thomas Jefferson University, Philadelphia, PA 19107, USA

[2]Jefferson Institute of Molecular Medicine, Thomas Jefferson University, Philadelphia, PA 19107, USA

[3]Department of Pathology and Cell Biology, Thomas Jefferson University, Philadelphia, PA 19107, USA

[4]Division of Rheumatology and Immunology, Medical University of South Carolina, Charleston, SC 29425, USA

Abstract

Objective—Examine whether lung endothelial cells (EC) from patients with Systemic Sclerosis (SSc)-associated interstitial lung disease (ILD) express mesenchymal cell-specific proteins and gene transcripts indicative of the occurrence of endothelial to mesenchymal (EndoMT) phenotypic transition.

Methods—Lung tissues from 6 patients with SSc-associated pulmonary fibrosis were examined by histopathology and immunohistochemistry. Confocal laser microscopy was employed to assess the simultaneous expression of EC and myofibroblast molecular markers. CD31+/CD102+ EC were isolated from lung tissues from two patients with SSc-associated ILD and from two normal lungs and the expression of EC and mesenchymal cell markers and other relevant genes were analyzed by quantitative PCR, immunofluorescence microscopy and Western blots.

Results—Immunohistochemistry showed cells expressing the EC-specific CD31 marker in sub-endothelial, perivascular and parenchymal regions of lungs from all SSc patients. Confocal microscopy identified cells displaying simultaneous expression of von Willebrand factor and α-smooth muscle actin in small and medium-sized arterioles in SSc lung tissues but not in control lungs. CD31+/CD102+ EC isolated from SSc lungs expressed high levels of mesenchymal cell-specific genes (collagen I, collagen III and fibronectin), EC-specific genes (collagen IV and VE-cadherin), profibrotic genes (TGF-β and CTGF), and genes encoding EndoMT-related transcription factors (TWIST1 and SNAI2).

Address all correspondence to: Sergio A. Jimenez, M.D., Jefferson Institute of Molecular Medicine, Thomas Jefferson University, 233 S. 10th Street, Room 509 BLSB, Philadelphia, PA 19107-5541, Phone: 215-503-5042, Fax: 215-923-4649, sergio.jimenez@jefferson.edu.

[5]Drs. Mendoza and Piera-Velazquez contributed equally to the studies described and both are first authors.

Conclusion—Cells co-expressing endothelial and mesenchymal cell-specific molecules are present in SSc-associated ILD lung tissues. CD31+/CD102+ EC isolated from SSc lungs expressed simultaneously mesenchymal and EC-specific transcripts and proteins. Collectively, these observations demonstrate the occurrence of EndoMT in lung tissues from patients with SSc-associated ILD.

Keywords

EndoMT; Systemic Sclerosis; Interstitial Lung Disease; Fibroblasts; Myofibroblast

INTRODUCTION

Systemic Sclerosis (SSc) is a systemic autoimmune disease of unknown etiology characterized by progressive fibrosis of skin and multiple internal organs, and severe fibroproliferative vasculopathy affecting the microvasculature resulting in severe vessel narrowing or even complete vascular obliteration (1–3). The pathogenetic mechanisms responsible for the fibrotic process and the severe vascular alterations in SSc are complex and have not been fully elucidated (4–6). Numerous recent studies have demonstrated that activated myofibroblasts are the cells ultimately responsible for the exaggerated deposition of extracellular matrix macromolecules in skin, the parenchyma of affected organs such as the lungs and the heart, and the subendothelial space of small and medium sized arteries in SSc (7–9). The activated myofibroblasts are a unique class of mesenchymal cells characterized by specific biological functions including a motile phenotype, expression of α-smooth muscle actin (α-SMA), increased production of fibrillar collagens type I (COL1) and type III (COL3), and reduction in the expression of genes encoding ECM-degradative enzymes (10,11).

The activated myofibroblasts in fibrotic tissues emerge from several sources (11–13), including expansion of resident tissue fibroblasts (14), migration and tissue accumulation of bone marrow-derived circulating fibrocytes (15,16), and from epithelial cells, pericytes, and Gli1-positive perivascular progenitor cells that have undergone transition to a mesenchymal phenotype (17–19). More recently, it has been demonstrated that endothelial cells (EC) are also capable of undergoing a phenotypic change into mesenchymal cells in a process known as endothelial to mesenchymal transition or EndoMT (20–23). Although EndoMT was initially considered to occur only during cardiovascular embryonic development (24), accumulating evidence indicates that this process occurs in various experimentally-induced models of tissue fibrosis (20–23,25–28), and may play a role in the pathogenesis of certain human fibrotic and vascular disorders, including Idiopathic and SSc-associated Pulmonary Arterial Hypertension (29–33). Here, we provide immunohistological and confocal microscopy evidence demonstrating that cells displaying specific EC molecular markers are present in the subendothelial, perivascular and parenchymal regions of lungs from patients with SSc-associated interstitial lung disease (ILD) and that EC expressing myofibroblast-specific molecular markers can be identified in the endothelium and subendothelial space of small and medium-sized arteries of SSc lungs. We further show that highly purified CD31+/CD102+ EC isolated from SSc-affected lungs produce numerous mesenchymal cell specific proteins and display the simultaneous expression of mesenchymal and EC-specific-

transcripts as well as the expression of EndoMT-associated transcription factors. These observations provide strong support to the hypothesis that a population of activated myofibroblasts responsible for the progressive intimal fibrosis, vascular occlusion and pulmonary fibrosis in SSc-associated ILD originate from lung EC through the EndoMT process. This novel mechanism may represent an important and novel therapeutic target for the severe and currently fatal complications of SSc–associated fibroproliferative vasculopathy and pulmonary fibrosis.

MATERIALS AND METHODS

Tissue samples

Lung tissues from six patients with SSc-associated ILD were studied. Two of the lung samples were from surgical open lung biopsies obtained at Thomas Jefferson University Hospital (Patients 1 and 2 in Table I) and the other four lung samples were from patients who had undergone lung transplantation at the University of Pittsburgh Medical Center. The surgical biopsies and the lung transplants were performed following informed consent and according to IRB approved protocols from Thomas Jefferson University and the University of Pittsburgh Medical Center. Two normal lung samples obtained at necropsy served as controls for all procedures. Both of the donors of normal lung tissues died from cerebrovascular accidents. One of the normal controls (Female, 55 years of age) was from the University of Pittsburgh Medical Center and lung tissues from the other (Female, 62 years of age) were obtained from the National Disease Research Interchange (NDRI, Philadelphia, PA). These two patients did not have a clinical history of pulmonary pathology and chest radiographs of both subjects obtained before their demise were normal.

Histopathology, immunohistochemistry and confocal laser microscopy

Paraffin embedded tissue slides were examined histopathologically employing hematoxylin-eosin and Masson's trichrome staining, and by immunohistochemical staining with specific endothelial and mesenchymal (myofibroblast) cell markers. The SSc and normal lung tissue samples were also examined by confocal laser microcopy as described previously (34). In all immunohistochemical and confocal laser microscopy studies samples incubated without primary antibody were used as negative controls. For immunohistochemistry the following primary antibodies were used: anti-CD31 (Neomarkers, Fremont, CA), anti-von Willebrand Factor (vWF, Dako, Denmark), anti-COL1 (Santa Cruz Biotechnology, Santa Cruz, CA), anti-COL3 (Fitzgerald, Acton, MA), and anti-α-SMA (Abcam, Cambridge, MA). For single antibody labeling, paraffin sections were immunoassayed by the peroxidase method using the indicated antibodies. For confocal laser microscopy paraffin samples were de-paraffinated and dehydrated following antigen retrieval with a citric acid buffer as described (34). Slides were first incubated with blocking IgG solution for 1 h and then overnight with one of the following antibodies: anti CD31 (1:50 dilution), anti α-SMA (1:200 dilution), anti-vWF (1:50 dilution), anti COL1 (1:200 dilution), or anti-COL3 (1:200 dilution) antibodies. IgG binding was revealed following incubation with (Fab′)-sheep anti-rabbit Cy3 antibody and (Fab′)-sheep anti-mouse FITC antibody (Sigma, St. Louis, MO) for 1 h. Nuclei were counterstained with 4,6-diamidino-2-phenylindole (DAPI, Jackson ImmunoResearch Laboratories, West Grove, PA). Samples were examined with a Zeiss 51 confocal laser

microscope (Zeiss, Thronwood, NY) to evaluate the co-localization of immunoreactivity with polyclonal and monoclonal antibodies in paired combinations of either CD31 or vWF with either α-SMA, COL1, or COL3.

Isolation of human lung EC

CD31+/CD102+ EC were isolated from the lungs of two patients with SSc-associated pulmonary fibrosis (Patients 3 and 4 on Table I) and from the two normal lungs employing a modification of previously published methods (35) as described previously (36). Briefly, lung tissue samples were minced with a scalpel and enzymatically digested with clostridial collagenase (30 mg/100ml in 0.1% BSA, Worthington, Lakewood, NJ) at 37°C for 1h to obtain a single cell suspension. Following removal of contaminating erythrocytes and inflammatory cells, the isolated cell suspension was employed for EC isolation and immunomagnetic selection with rabbit anti-human CD31 antibody followed by magnetic bead separation using goat anti-rabbit IgG-conjugated microbeads (1:5, Miltenyi Biotec). The isolated CD31+ EC were cultured in EC culture medium (ScienCell Research Laboratories, Carlsbad, CA) containing 5% FBS, 100 U/ml penicillin and 100 μg/ml streptomycin in 2% gelatin pre-coated tissue culture dishes for 5–10 days. Following expansion, the cells were re-suspended and further purified employing a second immunologic separation using rabbit anti-human CD102 antibody to obtain a highly purified preparation of CD31+/CD102+ EC. The purified CD31+/CD102+ EC were plated on 2% gelatin coated plastic dishes, their morphology assessed by phase contrast microscopy, and their EC phenotype confirmed by evaluating the cellular uptake of 1,1′-dioctadecyl-3,3,3′,3′-tetramethylindocarbocyanine perchlorate (Dil)-acetylated LDL (Dil-AcLDL, Biomedical Technologies, Stoughton, MA) as previously described (36). To further evaluate the EC-specific functional activity of the CD31+/CD102+ cells isolated from the SSc lungs the cells were cultured on plates coated with Matrigel (BD Bioscience, Bedford, MA) at 37°C in a 5% CO_2 atmosphere and microtube formation was examined during a 12 day culture period. All studies were performed with cells in early passage (less than passage 5) to assure the preservation of their original phenotype.

Immunofluorescence staining

For indirect immunofluorescence CD31+/CD102+ lung EC were seeded onto glass culture slides and were fixed with 3.7% formaldehyde and permeabilized with 0.1% Triton X-100 in PBS for 3 min. Slides were washed with PBS and blocked with PBS containing 1% BSA at room temperature for 1 h, and then they were incubated with primary antibodies against α-SMA (1:200 dilution), CD31 (1:50 dilution) and vWF (1:50 dilution). In other studies EC monolayers were examined by immunofluorescence with antibodies to the EC-specific marker VE-cadherin (1:100 dilution; Cell Signaling, Danvers, MA). Slides were then incubated with Cy3-conjugated secondary antibodies (1:500) followed by DAPI for nuclear staining.

Western blot analysis

Aliquots of CD31+/CD102+ lung EC culture media were processed for Western blot under denaturing conditions. Equal volume aliquots of culture media were resolved by SDS-polyacrylamide gel electrophoresis, and transferred to nitrocellulose membranes (Invitrogen,

Carlsbad, CA). Blots were blocked for 1 h in Odyssey Blocking buffer (LI-COR, Lincoln, NE). The membranes were then incubated overnight at 4°C with a polyclonal anti-COL1 antibody (Southern Biotech, Birmingham, AL), or a polyclonal anti-COL3 antibody (Sigma-Aldrich, St. Louis, MO) in the same blocking buffer. Membranes were then washed with PBS-Tween (PBS, 0.2% Tween 20), and incubated for 1 h with the appropriate horseradish peroxidase-conjugated secondary antibodies (GE Healthcare, UK) diluted 10,000-fold in Odyssey Blocking buffer. Signals were detected and quantitated employing the Odyssey Imagen System (LI-COR). For quantitative analysis of the Western blots the intensity of fluorescence of the protein bands was corrected for the amount of DNA (μg) in the corresponding tissue culture plates, representing the number of cells that were used to obtain the samples.

Quantitative reverse transcription (RT)-PCR

CD31+/CD102+ lung EC preparations from two normal and two SSc-associated ILD samples were cultured in duplicate wells of 12 well gelatin-treated plastic tissue culture dishes for 72 h and harvested with a cell lifter, washed in cold PBS and processed for RNA extraction (RNeasy kit; Qiagen, Valencia, CA) including a genomic DNA digestion step. Total RNA (1μg) was reverse-transcribed using Superscript II reverse transcriptase (Invitrogen, Carlsbad, CA) to generate first strand cDNA. EC transcript levels were quantified using SYBR Green real time PCR as described (37). The primers employed are listed in Supplementary Table I. The number of mRNA copies in each PCR was corrected for the 18S endogenous control transcript levels. The specificity of the primers was established at the end of the PCR amplification employing melt curve analyses.

Statistical analysis

Comparative CT (ΔΔCt) analysis was performed employing DataAssist 3.0 Software (Applied Biosystems) as described previously (37). The data obtained from SSc lung EC from each of the two patients was compared with the average of the data obtained from the two normal lung EC preparations and expressed as fold change.

RESULTS

Clinical and demographic characteristics of SSc-associated ILD patients studied

The clinical features of the SSc patients whose lung tissues were studied are shown in Table I. None of the patients had clinical features of pulmonary arterial hypertension at the time the tissue samples were obtained. All patients were tested for the presence of pulmonary arterial hypertension employing transthoracic echocardiograms and the four patients who underwent lung transplantation also had right heart catheterizations. None of the echocardiograms and right heart catheterization studies showed any evidence of pulmonary arterial hypertension at the time the lung biopsy sample was obtained.

Histopathology and immunohistology

All six lung tissue samples from the SSc-associated ILD patients displayed varying degrees of interstitial fibrosis along with a mononuclear cell inflammatory infiltrate pattern. Numerous small and medium size arteries in all samples showed marked intimal

proliferation resulting in narrowing of the vessel lumen and sometimes complete obliteration of the affected vessel as illustrated in Figure 1A. The endothelial cell marker CD31 was employed to identify EC present in the lung tissues by immunohistology. As expected, CD31 positive cells were found lining the vessel lumens as illustrated in Figures 1B–F. However, CD31 positive cells were also observed beneath the endothelial layer embedded within the subendothelial space which contained numerous elongated mesenchymal cells (Figures 1B and 1C), as well as in the perivascular tissue and within the lung parenchyma as illustrated in Figures 1D–F. These alterations were present in all the SSc-associated ILD samples examined as illustrated for SSc patient 2 (Figures 1B–D), patient 3 (Figure 1E), and patient 5 (Figure 1F), however, they were not present in the normal lung tissues (not shown).

Confocal laser microscopy

Confocal laser microscopy showed co-localization of vWF with α-SMA in the endothelium and within the subendothelial compartment in all SSc-associated ILD samples (Figure 2A). In contrast, samples from normal controls did not show any cells co-expressing the endothelial and mesenchymal cell markers (not shown). The co-localization of vWF and α-SMA was observed in both small and medium sized arterioles, however, it was quite heterogeneous with some vessels displaying numerous EC co-expressing both markers as illustrated in Figure 2A, whereas, in other vessels there were only a few or none. Owing to this heterogeneity it was not possible to obtain an accurate quantitative assessment of the frequence of cells co-expressing both endothelial and mesenchymal cell markers in the SSc lung tissues. We also observed that in contrast with normal lungs (illustrated in Figure 2D), in SSc-lungs the EC layer of numerous vessels displayed areas of detachment from the vessel wall (Figure 2E, arrow) and in some vessels variable portions of vessel lumen appeared completely denuded from endothelial lining as illustrated in Figure 2E (arrowheads). Also, most EC in the SSc tissues displayed very weak or absent CD31 staining (Figure 2E,F) compared with the very intense CD31 staining in the vessels in the control lungs (Figure 2D). Marked sub-endothelial accumulation of COL1 (not shown) and COL3 (Figures 2E,F) was also observed with various degrees of severity in all small and medium size arterioles throughout the SSc tissues.

Indirect immunofluorescence of CD31+/CD102+ lung EC and *in vitro* microtube formation

To confirm the purity of the EC isolated from the SSc lungs dark field microcopy, indirect immunofluorescence, and microtube formation analysis of the cultured CD31+/CD102+ EC from SSc lungs were performed. Dark field microscopy showed the typical EC cobblestone morphology in monolayer cultures and immunofluorescence demonstrated intense staining for the EC-specific marker VE-cadherin (Figure 3A) essentially in all cells confirming the high level of EC purity in the samples studied. Furthermore, culture of the cells on a Matrigel substrate resulted in the formation of numerous microtubes indicative of the preservation of EC functional activities by the purified cells (Figure 3B).

Gene expression and Western blot analysis of CD31+/CD102+ lung EC

The gene expression assessment of immunopurified CD31+/CD102+ EC obtained from lung tissues from two patients with SSc-associated ILD compared to the average gene expression of immunopurified CD31+/CD102+ EC from two normal lungs is shown in Figure 4A. The

results demonstrated a very strong expression of COL1A1 and COL3A1 in the CD31+/CD102+ purified EC from lungs from SSc patients with values up to 21 times and 26 times higher, respectively, than the expression of the same collagen genes in CD31+/CD102+ EC purified from the normal lungs. The expression of FN1 and ACTA2 (α-SMA) and other profibrotic genes such as TGFB1 and CTGF, as well as the expression of several EndoMT-related genes such as SNAI2 and TWIST1 was also substantially increased in the CD31+/CD102+ EC from the lungs of SSc patients (Figure 4A). Western blots of the culture media from CD31+/CD102+ EC isolated from the two SSc lungs confirmed the gene expression results showing statistically significant greater amounts of type I and type III collagens compared to samples of culture media from the CD31+/CD102+ EC isolated from the two normal lungs (Figure 4B).

DISCUSSION

The generation of activated myofibroblasts, which are distinguished from quiescent resident fibroblasts by the initiation of expression of α-SMA and the increased production of fibrillar type I and type III collagens (9–11), is a crucial mechanism in the development of tissue fibrosis in SSc (7–9). Recently, EndoMT has been recognized as an important mechanism in the generation of activated myofibroblasts involved in the development of several experimentally-induced tissue fibrosis animal models (20–23,25–28) as well as in some fibrotic human diseases (29–33). Despite its potential role in pathogenesis of numerous human disorders the detailed mechanisms involved in EndoMT have not been fully elucidated, although the crucial role of TGF-β in its initiation and maintenance, as well as the participation of several transcription factors involved in cellular transdifferentiation including SNAI1, SNAI2 or SLUG, and TWIST1 has been well documented (20–23, 38,39).

Here, we provide immunohistopathological evidence of the presence of cells expressing EC-specific molecular markers in the subendothelial neointima as well as in the perivascular regions and in the parenchyma of lung tissues from patients with SSc-associated ILD. Furthermore, we describe confocal microscopy studies demonstrating the presence of numerous cells simultaneously expressing endothelial and mesenchymal cell molecular markers in small and medium-sized arterioles within the SSc lungs. Similar findings were recently described in pulmonary arteries of patients with primary pulmonary artery hypertension (32), as well as in arterioles of patients with SSc-associated pulmonary hypertension (33) but were not present in pulmonary vessels from healthy controls (32,33). The frequency of cells co-expressing EC and myofibroblast markers was assessed in the lung microvasculature of patients with SSc-associated pulmonary hypertension and was found to occur in less than 5% of EC in pulmonary arterioles (33). In our study we found that the frequency of cells expressing simultaneously endothelial and mesenchymal cell-specific markers was substantially higher, although their occurrence was quite heterogeneous with some vessels showing that essentially all EC co-expressed vWF and α-SMA as illustrated in Figure 2A–C, whereas other vessels contained only few EC displaying co-expression and still other vessels that did not show any EC co-expressing vWF and α-SMA staining. However, owing to the heterogeneity of co-expression on the vessels examined, the low intensity of staining for EC-specific markers in most SSc cells, and the frequent occurrence in SSc lung tissues of abundant and quite variable numbers of

inflammatory cells in the subendothelial and perivascular regions it was not possible to provide an accurate quantitation of the frequency of cells displaying EndoMT in SSc-associated ILD. An important observation described here is that immunopurified CD31+/CD102+ lung EC isolated and expanded *in vitro* from lung tissues from patients with SSc-associated ILD exhibited marked up-regulation in the expression and production of interstitial type I and type III collagens, and increased levels of transcripts for the potent profibrotic growth factors, TGF-β and CTGF. These cells also expressed high levels of transcripts for several other EndoMT related proteins, such as the transcription factors TWIST1 and SNAI2. The marked increase in the expression of TWIST1 in CD31+/CD102+ EC isolated from SSc lungs we observed in our study is similar to that found in explanted lung EC from patients with idiopathic pulmonary artery hypertension, a finding that was considered to indicate the occurrence of TWIST1-driven EndoMT *in vivo* (32).

Collectively, the novel observations described in our study provide strong evidence for the occurrence of EndoMT in small and medium size arterioles of lung tissues from patients with SSc-associated ILD, and suggest that EndoMT may play a role in the development of the severe fibroproliferative vasculopathy and progressive parenchymal fibrosis that are the hallmarks of the pulmonary involvement in SSc (40–42). These results also suggest that greater understanding of the molecular mechanisms involved in EndoMT and its pharmacological modulation may represent a novel therapeutic approach for the fibroproliferative vasculopathy of SSc-associated tissue fibrosis.

Supplementary Material

Refer to Web version on PubMed Central for supplementary material.

Acknowledgments

Supported by the National Institute of Arthritis and Musculoskeletal and Skin Diseases, part of the National Institutes of Health, under Award Number R01 AR19616, “Biochemical and Vascular Alterations in Scleroderma” to SAJ, Award Number P30 AR061271 Core Center to CFB, and Award Number K24 AR060297 to CFB. The content is solely the responsibility of the authors and does not necessarily represent the official views of the National Institutes of Health. The expert technical assistance of Alma Makul and Kerri Fasino, and the assistance of Kenneth Brown, Matthew Landmesser, and Ruth Johnson in the preparation of this manuscript are duly acknowledged.

References

1. Varga J, Abraham D. Systemic sclerosis: a prototypic multisystem fibrotic disorder. J Clin Invest. 2007; 117:557–67. [PubMed: 17332883]
2. Gabrielli A, Avvedimento EV, Krieg T. Scleroderma. N Engl J Med. 2009; 360:1989–2003. [PubMed: 19420368]
3. Matucci-Cerinic M, Kahaleh B, Wigley FM. Systemic Sclerosis (scleroderma, SSc) is a vascular disease. Arthritis Rheum. 2013; 65:1953–62. [PubMed: 23666787]
4. Jimenez SA, Derk CT. Following the molecular pathways toward an understanding of the pathogenesis of Systemic Sclerosis. Ann Int Med. 2004; 140:37–50. [PubMed: 14706971]
5. Katsumoto TR, Whitfield ML, Connolly MK. The pathogenesis of systemic sclerosis. Annu Rev Pathol. 2011; 6:509–37. [PubMed: 21090968]
6. Pattanaik D, Brown M, Postlethwaite BC, Postlethwaite AE. Pathogenesis of Systemic Sclerosis. Front Immunol. 2015; 6:272. [PubMed: 26106387]

7. Beon M, Harley RA, Wessels A, Silver RM, Ludwicka-Bradley A. Myofibroblast induction and microvascular alteration in scleroderma lung fibrosis. Clin Exp Rheumatol. 2004; 22:733–42. [PubMed: 15638048]
8. Gilbane AJ, Denton CP, Holmes AM. Scleroderma pathogenesis: a pivotal role for fibroblasts as effector cells. Arthritis Res Ther. 2013 Jun 17.15(3):215. [PubMed: 23796020]
9. Kendall RT, Feghali-Bostwick CA. Fibroblasts in fibrosis: novel roles and mediators. Front Pharmacol. 2014; 5:123. [PubMed: 24904424]
10. Hinz B, Phan SH, Thannickal VJ, Prunotto M, Desmoulière A, Varga J, et al. Recent developments in myofibroblast biology: paradigms for connective tissue remodeling. Am J Pathol. 2012; 180:1340–55. [PubMed: 22387320]
11. Hinz B, Phan SH, Thannickal VJ, Galli A, Bochaton-Piallat ML, Gabbiani G. The myofibroblast: one function, multiple origins. Am J Pathol. 2007; 170:1807–16. [PubMed: 17525249]
12. McAnulty RJ. Fibroblasts and myofibroblasts: their source, function and role in disease. Int J Biochem Cell Biol. 2007; 39:666–71. [PubMed: 17196874]
13. Falke LL, Gholizadeh S, Goldschmeding R, Kok RJ, Nguyen TQ. Diverse origins of the myofibroblast-implications for kidney fibrosis. Nat Rev Nephrol. 2015; 11:233–44. [PubMed: 25584804]
14. Poslethwaite AE, Shigemitsu H, Kanagat S. Cellular origins of fibroblasts: possible implications for organ fibrosis in systemic sclerosis. Curr Opin Rheumatol. 2004; 16:733–8. [PubMed: 15577612]
15. Strieter RM, Keeley EC, Hughes MA, Burdick MD, Mehrad B. The role of circulating mesenchymal progenitor cells (fibrocytes) in the pathogenesis of pulmonary fibrosis. J Leukoc Biol. 2009; 86:1111–8. [PubMed: 19581373]
16. Herzog EL, Bucala R. Fibrocytes in health and disease. Exp Hematol. 2010; 38:548–556. [PubMed: 20303382]
17. Lamouille S, Xu J, Derynck R. Molecular mechanisms of epithelial-mesenchymal transition. Nat Rev Mol Cell Biol. 2014; 15:178–96. [PubMed: 24556840]
18. Humphreys BD, Lin SL, Kobayashi A, Hudson TE, Nowlin BT, Bonventre JV, et al. Fate tracing reveals the pericyte and not epithelial origin on myofibroblasts in kidney fibrosis. Am J Pathol. 2010; 176:85–97. [PubMed: 20008127]
19. Kramann R, Schneider RK, DiRocco DP, Machado F, Fleig S, Bondzie PA, et al. Perivascular Gli1+ progenitors are key contributors to injury-induced organ fibrosis. Cell Stem Cell. 2015; 16:51–66. [PubMed: 25465115]
20. Zeisberg EM, Taranavski O, Zeisberg M, Dorfman AL, McMullen JR, Gustafsson E, et al. Endothelial-to-mesenchymal transition contributes to cardiac fibrosis. Nat Med. 2007; 13:952–61. [PubMed: 17660828]
21. Goumans MJ, van Zonneveld AJ, ten Dijke P. Transforming growth factor β-induced endothelial-to-mesenchymal transition: A switch to cardiac fibrosis? Trends Cardiovasc Med. 2008; 18:293–8. [PubMed: 19345316]
22. Piera-Velazquez S, Li Z, Jimenez SA. Role of Endothelial-Mesenchymal Transition (EndoMT) in the Pathogenesis of Fibrotic Disorders. Am J Pathol. 2011; 179:1074–84. [PubMed: 21763673]
23. Piera-Velazquez S, Jimenez SA. Molecular mechanisms of endothelial to mesenchymal cell transition (EndoMT) in experimentally induced fibrotic diseases. Fibrogenesis Tissue Repair. 2012; 5 (Suppl 1):S7. [PubMed: 23259736]
24. Arciniegas E, Neves CY, Carrillo LM, Zambrano EA, Ramirez R. Endothelial-mesenchymal transition occurs during embryonic pulmonary artery development. Endothelium. 2005; 12:193–200. [PubMed: 16162442]
25. Zeisberg EM, Potenta SE, Sugimoto H, Zeisberg M, Kalluri R. Fibroblasts in kidney fibrosis emerge via endothelial-to-mesenchymal transition. J Am Soc Nephrol. 2008; 19:2282–7. [PubMed: 18987304]
26. Li J, Qu X, Bertman JF. Endothelial-Myofibroblast Transition Contributes to the Early Development of Diabetic Renal Interstitial Fibrosis in Streptozotocin-Induced Diabetic Mice. Am J Pathol. 2009; 175:1380–8. [PubMed: 19729486]

27. Hashimoto N, Phan SH, Imaizumi K, Matsuo M, Nakashima H, Kawabe T, et al. Endothelial-mesenchymal transition in bleomycin-induced pulmonary fibrosis. Am J Respir Cell Mol Biol. 2010; 43:161–72. [PubMed: 19767450]
28. LeBleu VS, Taduri G, O'Connell J, Teng Y, Cooke VG, Woda C, et al. Origin and function of myofibroblasts in kidney fibrosis. Nat Med. 2012; 19:1047–53. [PubMed: 23817022]
29. Rieder F, Kessler SP, West GA, Bhilocha S, de la Motte C, Sadler TM, et al. Inflammation-induced endothelial-to-mesenchymal transition: a novel mechanism of interstitial fibrosis. Am J Pathol. 2011; 179:2660–73. [PubMed: 21945322]
30. Yoshimatsu Y, Watabe T. Roles of TGF-β signals in endothelial-mesenchymal transition during cardiac fibrosis. Int J Inflam. 2011:724080. [PubMed: 22187661]
31. Cooley BC, Nevado J, Mellad J, Yang D, St Hilaire C, Negro A, et al. TGF-β signaling mediates endothelial-to mesenchymal transition (EndMT) during vein graft remodeling. Sci Transl Med. 2014; 6:227ra34.
32. Ranchoux B, Antigny F, Rucker-Martin C, Hautefort A, Péchoux C, Bogaard HJ, et al. Endothelial-to-mesenchymal transition in pulmonary hypertension. Circulation. 2015 pii:CIRCULATIONAHA.114.008750 Epub ahead of print.
33. Good RB, Gilbane AJ, Trinder SL, Denton CP, Coghlan G, Abraham DJ, et al. Endothelial to Mesenchymal Transition Contributes to Endothelial Dysfunction in Pulmonary Arterial Hypertension. Am J Pathol. 2015; 185:1850–8. [PubMed: 25956031]
34. Del Galdo F, Sotgia F, de Almeida CJ, Jasmin JF, Musick M, Lisanti MP, et al. Decreased expression of caveolin 1 in patients with systemic sclerosis: crucial role in the pathogenesis of tissue fibrosis. Arthritis Rheum. 2008; 58:2854–65. [PubMed: 18759267]
35. Marelli-Berg FM, Peek E, Lidington EA, Stauss HJ, Lechler RI. Isolation of endothelial cells from murine tissue. J Immunol Methods. 2000; 244:205–15. [PubMed: 11033033]
36. Li Z, Jimenez SA. Protein Kinase Cδ and c-Abl kinase are required for transforming growth factor β induction of endothelial-mesenchymal transition in vitro. Arthritis Rheum. 2011; 63:2473–83. [PubMed: 21425122]
37. Nolan T, Hands RE, Bustin SA. Quantification of mRNA using real-time RT-PCR. Nat Protoc. 2006; 1:1559–82. [PubMed: 17406449]
38. Medici D, Potenta S, Kalluri R. Transforming growth factor-β2 promotes Snail-mediated endothelial mesenchymal transition through convergence of Smad-dependent and Smad-independent signaling. Biochem J. 2011; 433:515–20. [PubMed: 21087211]
39. van Meeteren LA, ten Dijke P. Regulation of endothelial cell plasticity by TGF-β. Cell Tissue Res. 2012; 347:177–86. [PubMed: 21866313]
40. Veraldi KL, Hsu E, Feghali-Bostwick CA. Pathogenesis of pulmonary fibrosis in systemic sclerosis: lessons from interstitial lung disease. Curr Rheumatol Rep. 2010; 12:19–25. [PubMed: 20425529]
41. Herzog EL, Mathur A, Tager AM, Feghali-Bostwick C, Schneider F, Varga J. Review: interstitial lung disease associated with systemic sclerosis and idiopathic pulmonary fibrosis: how similar and distinct? Arthritis Rheumatol. 2014; 66:1967–78. [PubMed: 24838199]
42. Wells AU, Margaritopoulos GA, Antoniou KM, Denton C. Interstitial lung disease in systemic sclerosis. Semin Respir Crit Care Med. 2014; 35:213–21. [PubMed: 24668536]

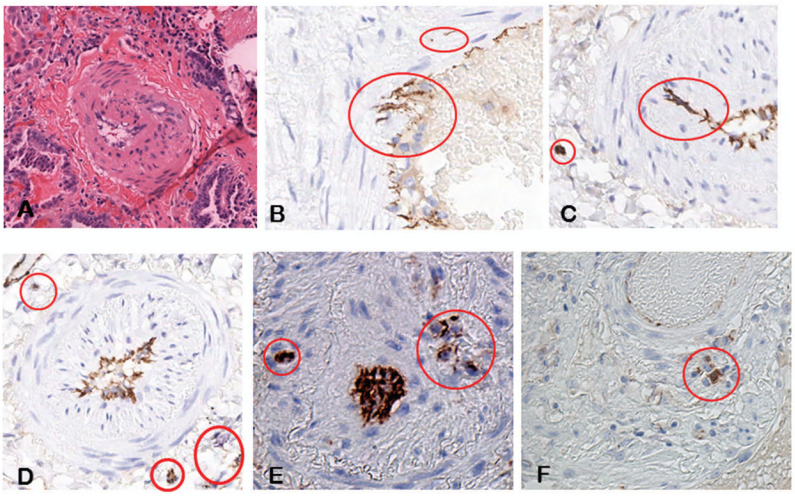

Figure 1. Histopathology and immunohistology of SSc-associated ILD lung tissues

A. A small artery in the lung of a patient with SSc-associated ILD stained with hematoxylin-eosin. Note the severe narrowing of the vessel lumen as a result of the accumulation of elongated mesenchymal cells and large amounts of fibrous tissue in the subendothelial intimal space. **B.** Immunohistochemical staining of the same tissue for the endothelial cell specific antibody marker CD31. Note the presence of CD31 positive cells in the subendothelial space besides their expected endothelial location. **C.** Lung tissue from another patient showing two cells bearing the EC-specific CD31 marker embedded within the neointimal tissue removed from the endothelium, and a CD31-positive cell cluster within the fibrotic lung parenchyma. **D-F.** CD31 immunohistological staining of lung tissues from three additional SSc patients showing similar findings.

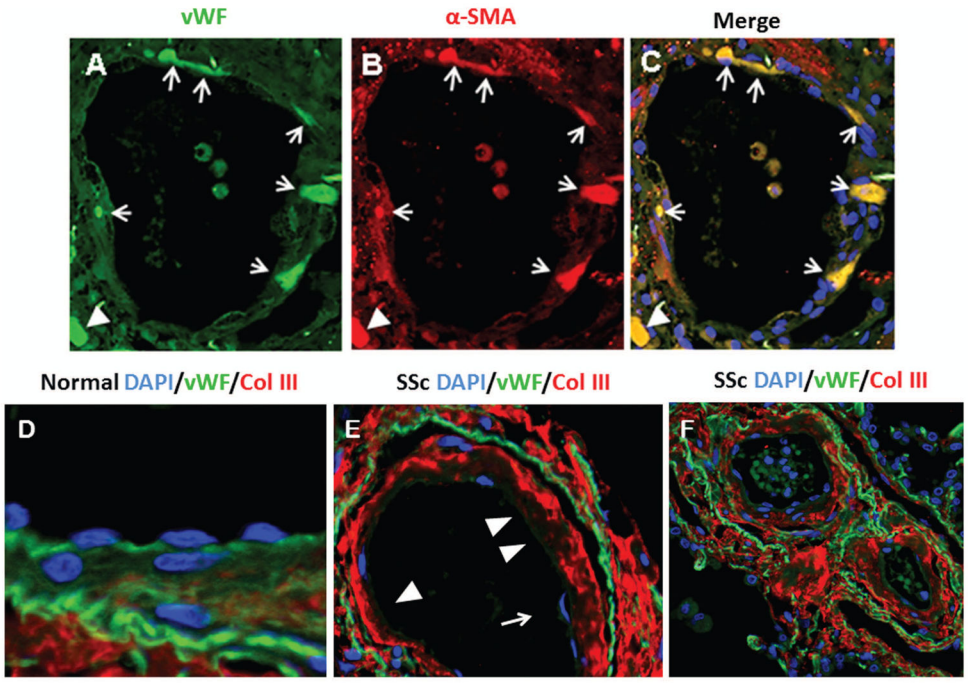

Figure 2. Confocal microscopy staining for vWF and α-SMA of a small arteriole in the lung of a patient with SSc-associated ILD and for COL3 and CD31 of medium-sized arterioles in normal lungs or in lung tissues from SSc-associated ILD

A. Staining for vWF shown in green; **B.** Staining for α-SMA shown in red; **C.** Cells co-expressing vWF and α-SMA are shown in yellow in the merged image. Note that essentially all the vWF-stained cells present within the endothelium and subendothelial tissue express the mesenchymal cell marker α-SMA. **D.** Confocal microscopy of medium-sized arteriole in normal lung stained for CD31 (green) and COL3 (red). Note intense endothelial CD31 staining. The endothelium appears continuous and well attached to the vessel wall structures. COL3 staining is only present beyond the elastic lamina. **E.** In SSc vessels the endothelial lining is detached from the vessel wall (arrow) and some areas of denuded endothelium are noticeable (arrowheads). CD31 staining is noticeably weaker in the endothelial layer in the SSc vessel compared to the normal vessel. **F.** Intense and abundant staining for COL3 in the subendothelial, medial, and adventitial layers of the SSc vessels.

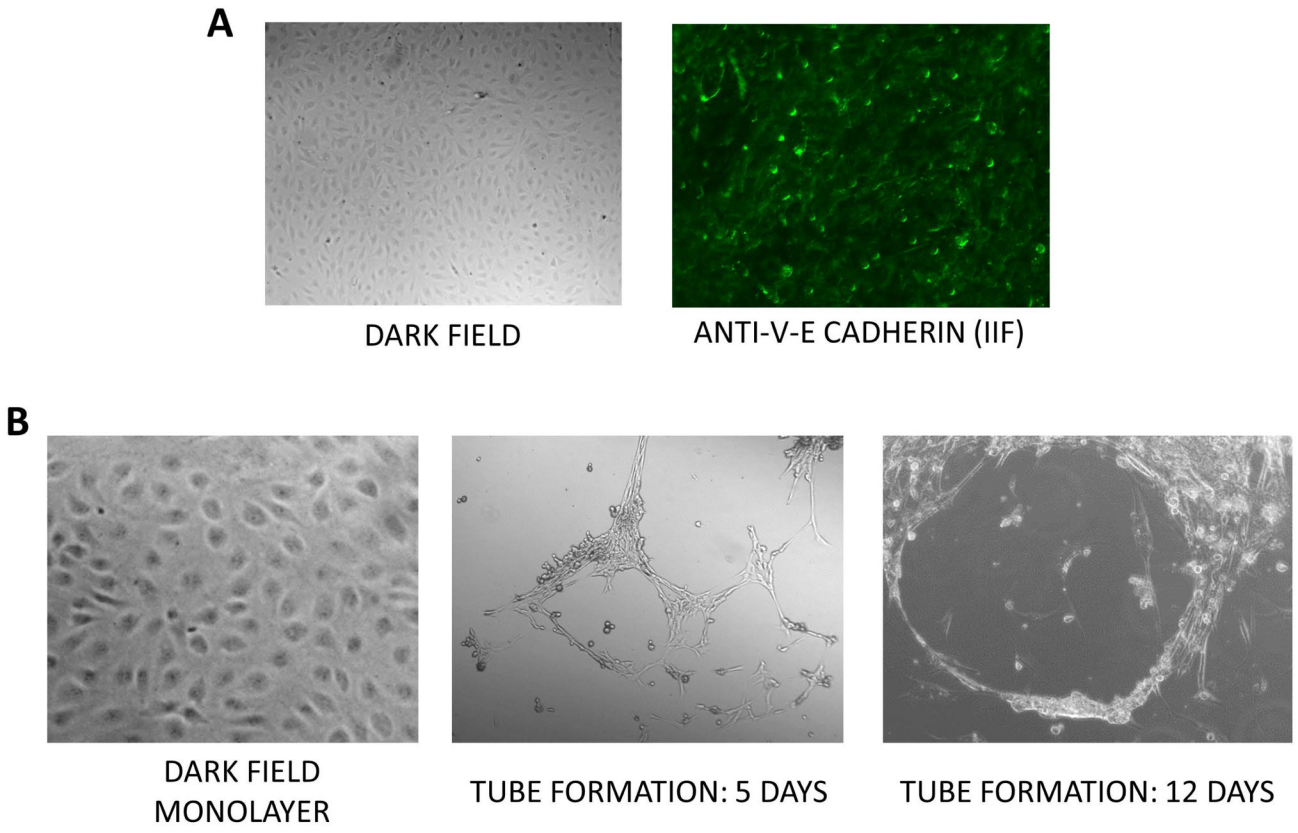

Figure 3. Morphologic and immunofluorescence analysis and *in vitro* microtube formation of cultured CD31+/CD102+ EC isolated from SSc tissues

A. Dark contrast microscope image (left panel) and immunofluorescence for VE-cadherin (right panel). **B.** Dark contrast microscope images of monolayer cultures (gelatin-coated, left panel) and following microtube formation in Matrigel culture at 5 and 12 days.

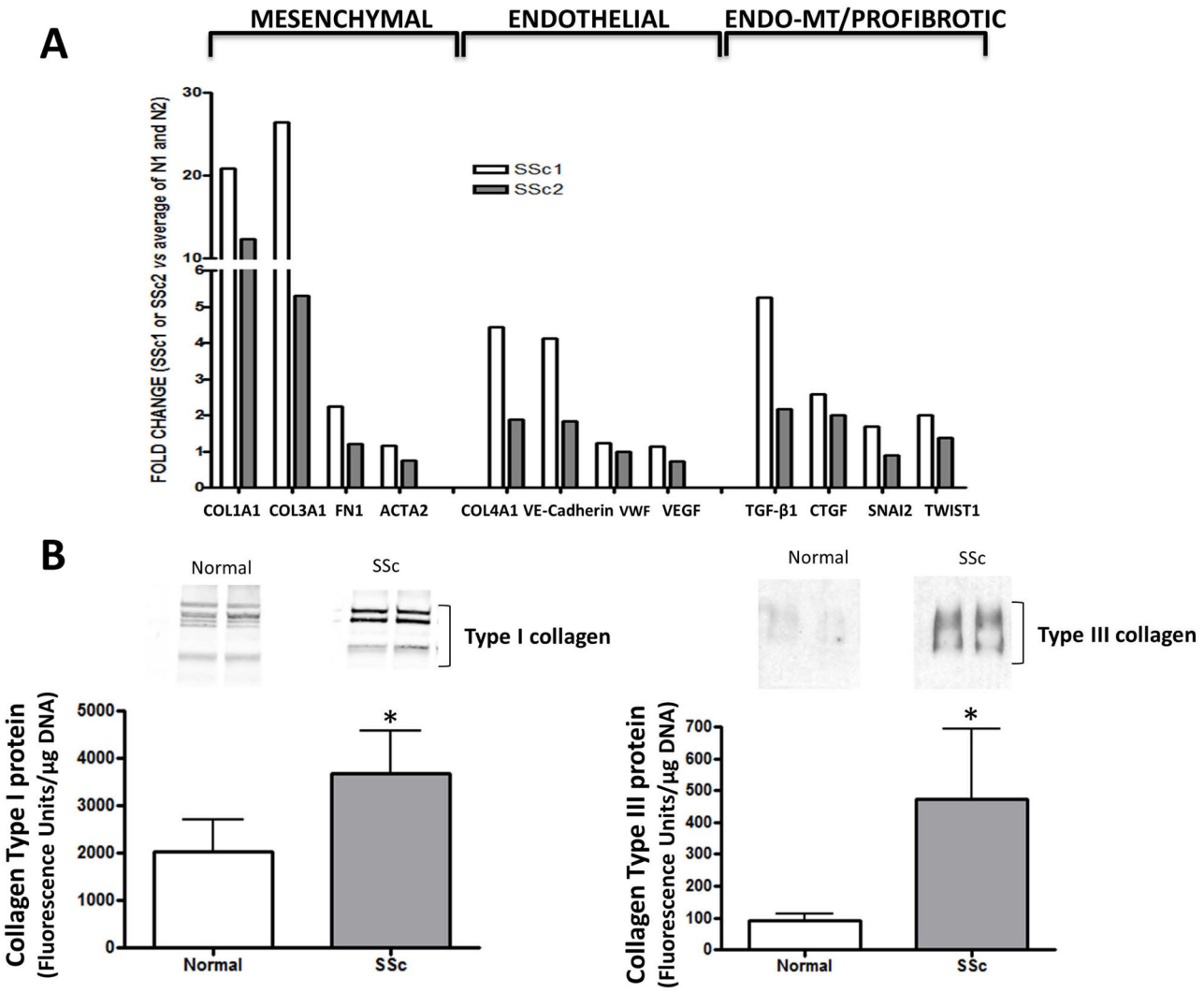

Figure 4. Quantitative PCR assessment and Western blot analysis of expression levels of selected genes and proteins in CD31+/CD102+ lung EC from SSc-associated ILD

A. Quantitative PCR of two different preparations of CD31+/CD102+ EC from lungs of two SSc patients or from normal lungs analyzed in duplicate. Shown are transcript measurements for interstitial collagen genes (COL1 and COL3), fibronectin 1 (FN1), α-SMA (SMA), EC-specific genes (COL4A1, VE-cadherin, vWF and VEGF), profibrotic genes (TGF-β1 and CTGF), and EndoMT-related transcription factors (SNAI2, and TWIST1). The vertical scale shows expression levels as fold change in CD31+/CD102+ EC from each of the SSc lungs (SSc1 and SSc2) compared to the average levels of the CD31+/CD102+ EC from the two normal lungs. **B.** Representative Western blots for secreted type I and type III collagens in culture media of CD31+/CD102+ EC from two normal and two SSc lungs. The bar graphs show a quantitative analysis of results from duplicate cultures of each cell line in three separate experiments expressed in units of fluorescence corrected for DNA content. *:p values for the difference between cells from SSc and control lungs were <0.05.

Table I

Selected clinical and demographic characteristics of Systemic Sclerosis Patients

Subject Number	**1**	**2**	**3**	**4**	**5**	**6**
SSc subtype	Diffuse	Limited	Unspecified	Unspecified	Unspecified	Unspecified
Type of sample	Biopsy	Biopsy	Transplant	Transplant	Transplant	Transplant
Age*	53	45	68	30	52	64
Gender	Male	Female	Female	Female	Female	Male
Time from skin disease onset	2 years	5 years	Unspecified	7 years	10 years	15 years
Time from respiratory symptoms onset	6 mo	8 mo	Unspecified	Unspecified	Unspecified	Unspecified
Smoking	No	No	No	No	No	Yes
Progressive respiratory symptoms	Yes	Yes	Yes	Yes	Yes	Yes
Pulmonary Hypertension	No	No**	No	No	No	No
ANA titer	1/640	1/640	Positive	Positive	Positive	Positive
Scl-70/ACA Antibodies	Negative	Centromere	N/A	N/A	N/A	N/A

*Age (in years) at the time of the sampling.

**Patient developed pulmonary hypertension 10 months after the lung biopsy was obtained.

Scl-70: Anti-topoisomerase antibodies.

ACA: Anti-centromere antibodies.

N/A: Not available.

Arthritis Rheumatol. Author manuscript; available in PMC 2017 January 01.